Clays and Clay Minerals, Vol. 40, No. 5, 561–566, 1992.

THE INTERLAYER COLLAPSE DURING DEHYDRATION OF SYNTHETIC $Na_{0.7}$-BEIDELLITE: A ^{23}Na SOLID-STATE MAGIC-ANGLE SPINNING NMR STUDY[1]

J. Theo Kloprogge, J. Ben H. Jansen, Roelof D. Schuiling, and John W. Geus[2]

Department of Geochemistry, Institute for Earth Sciences, University of Utrecht
Budapestlaan 4, P.O. Box 80.021, 3508 TA Utrecht, The Netherlands

[2] Department of Inorganic Chemistry, University of Utrecht
P.O. Box 80083, 3508 TB Utrecht, The Netherlands

Abstract—The dehydration and migration of the interlayer cation of the synthetic beidellite $Na_{0.7}Al_{4.7}Si_{7.3}O_{20}(OH)_4 \cdot nH_2O$, were studied with solid-state ^{23}Na and ^{27}Al MAS-NMR, heating stage XRD, and thermogravimetric analyses (TGA, DTA). The ^{23}Na MAS-NMR of Na-beidellite at 25°C displays a chemical shift of 0.2 ppm, which indicates a configuration comparable with that of Na^+ in solution. Total dehydration proceeds reversibly in two temperature ranges. Four water molecules per Na^+ are gradually removed from 25° to 85°C. As a result, the basal spacing decreases from 12.54 Å to 9.98 Å and the Na^+ surrounded by the two remaining water molecules is relocated in the hexagonal cavities of the tetrahedral sheet. The chemical shift of 1.5 ppm exhibited after the first dehydration stage illustrates the increased influence of the tetrahedral sheet. The high local symmetry is maintained throughout the entire first dehydration stage. During the second dehydration, which proceeds in a narrow temperature range around 400°C, the remaining two water molecules are removed reversibly without any change of the basal spacing.

Key Words—Beidellite, Dehydration, Interlayer collapse, ^{23}Na MAS-NMR.

INTRODUCTION

In the last decade, pillared smectites were increasingly studied for their possible use as catalysts and molecular sieves. The nature of the interlayer cation and its hydration shell largely determine properties such as swelling, cation exchange, and catalytic activity, e.g., in oil cracking reactions.

Dehydration reactions provide important information about the interlayer configuration. With the synthetic beidellite $Na_{0.7}Al_{4.7}Si_{7.3}O_{20}(OH)_4 \cdot nH_2O$, Kloprogge *et al.* (1990a) observed one main dehydration reaction occurring below 55°C, followed by a slow but continuous dehydration up to approximately 400°C. Experimental studies by Koster van Groos and Guggenheim (1984, 1986, 1987) have demonstrated that montmorillonite dehydrates in two stages. The two dehydration steps were interpreted as dehydration of a voluminous, but weakly bonded, outer hydration shell around the interlayer cation, and of a more strongly bonded inner hydration shell at approximately 140° to 150°C and 200° to 210°C, respectively.

Solid-state magic-angle spinning nuclear magnetic resonance (MAS-NMR) on zeolites and clays is a powerful technique to elucidate the structural environment of exchangeable cations such as ^{7}Li, ^{23}Na (Janssen *et al.*, 1989a, 1989b), ^{113}Cd (Bank *et al.*, 1989), and ^{133}Cs (Chu *et al.*, 1987; Kirkpatrick, 1988; Weiss *et al.*, 1990a, 1990b). ^{23}Na MAS-NMR has been applied to zeolites, sodium-feldspars (Kirkpatrick *et al.*, 1985; Yang *et al.*, 1986) and framework aluminosilicate glasses (Oestrike *et al.*, 1987). Most of the structural information is gathered from the ^{23}Na chemical shifts and from the changes in the second order quadrupole interactions.

The purpose of the present study is to elucidate the interlayer geometry of Na-beidellite during dehydration. Knowledge of the interlayer geometry as a function of the extent of dehydration may provide insight on phenomena proceeding during pillaring of synthetic Na-beidellite. More particularly, information may be gained concerning the position of the pillars and the structural relation with the tetrahedral sheets of the clay. Therefore, ^{23}Na and ^{27}Al magic-angle spinning nuclear magnetic resonance (MAS-NMR) is performed in experiments in which the Na-beidellite is heated to 105°C. For refinement of the interpretation, the results are combined with thermogravimetric (TGA) and differential thermal analysis (DTA) up to 1100°C, and heating stage X-ray diffraction (HT-XRD) up to 400°C.

EXPERIMENTAL METHODS

Samples

Na-beidellite, $Na_{0.7}Al_{4.7}Si_{7.3}O_{20}(OH)_4 \cdot nH_2O$, is hydrothermally synthesized from a stoichiometric gel prepared according to the method of Hamilton and Henderson (1968). The synthesis is performed at 350°C and 1 kbar in a Tuttle-type, externally heated, cold-seal pressure vessel (Tuttle, 1949). Kloprogge *et al.*

[1] Publication of the Debye Institute, University of Utrecht, The Netherlands.

Table 1. Chemical composition, unit cell parameters, and ^{27}Al and ^{29}Si MAS-NMR chemical shifts of the synthetic Na-beidellite (Kloprogge *et al.*, 1990a, 1990b).

	Chemistry		X-ray diffraction	Solid-state MAS-NMR			
				^{27}Al		^{29}Si	
	Wt. %	Formula (22 O)	Unit cell[1] parameters (Å)	δ (ppm)	I	δ (ppm)	I
SiO_2	56.76	Si 7.3	a 5.18 ± 0.005	[4]Al 69.9	0.25	Si(0Al) −92.7	0.61
Al_2O_3	30.96	Al 4.7	b 8.96 ± 0.008	[6]Al 3.9	0.75	Si(1Al) −88.4	0.29
Na_2O	2.44	Na 0.6	c 12.54 ± 0.011			Si(2Al) −82.3	0.10
H_2O	9.65						

[1] Orthorhombic cell (Kloprogge *et al.*, 1990a).

(1990a, 1990b) have reported on the synthesis procedure and product characterization. The samples are dried overnight at 120°C and rehydrated in air of approximately 60% relative humidity before the dehydration experiments. A summary of selected mineralogical data is given in Table 1.

Analytical techniques

A Du Pont 1090 analyzer was used for TGA, DTG, and DTA, applying heating rates of 0.5°C/min and 10°C/min within a N_2 flow. Approximately 20 mg of clay were used for these experiments. Heating stage X-ray powder diffraction was carried out with CuKα_1, in an HT Guinier (Enraf Nonius FR553) focusing powder camera, applying a heating rate of 0.5°C/min. ^{23}Na, ^{27}Al, and ^{29}Si MAS-NMR spectra were recorded on a Bruker WM500 (11.7 Tesla) at 132.258, 130.321, and 99.346 MHz, respectively, at the Department of Physical Chemistry, University of Nijmegen. The pulse width was 3.0 μsec for both Al and Na. The samples were spun at a frequency of approximately 10.5 kHz for Al and Si NMR, and 3 kHz for Na NMR. Standard 256 Free Induction Decays (FIDs) were accumulated at a repetition time of 1 s. Chemical shifts are reported in ppm relative to a NaCl solution for ^{23}Na and to $Al(H_2O)_6^{3+}$ for ^{27}Al.

RESULTS

At a relative humidity of 60%, HT-XRD of randomly oriented samples reveals a collapse of the interlayer spacing in the temperature range of 20° to 54°C. The d_{001} and d_{002} decrease from 12.54 Å and 6.27 Å at 20°C to 9.98 Å and 4.99 Å at 54°C, respectively. The intensity of the (004) reflection decreases in this temperature interval and ultimately disappears, whereas the (003) reflection becomes stronger (Figure 1). Up to 400°C the basal spacing remains constant.

The collapse of the interlayer spacing coincides with a strong weight loss of 6.6% below 85°C as confirmed by TGA (Figure 2A), applying the same heating rate (0.5°C/min) as in the HT-XRD. Between 85° and 400°C an additional amount of 2.6 wt. % water is gradually lost. The DTA curve exhibits one strong endothermic peak at 80°C (Figure 2B).

A water resorption experiment was performed in a TGA-balance after dehydration up to 400°C, followed by cooling to 25°C and keeping the sample at 25°C for 1400 min. The Na-beidellite resorbs water until a constant weight is reached after 1300 min (Figure 3). An amount equal to 2.16 moles water is adsorbed per mole Na-beidellite in air with a relative humidity of approximately 60%. XRD of the resorbed Na-beidellite reveals a rapid recovery of the basal spacing to 12.44 Å after approximately 45 min.

^{23}Na MAS-NMR spectra of Na-beidellite exhibit one sharp resonance near 0 ppm (Figure 4A). No doublets typical of relatively large second order quadrupole interactions are observed. Upon dehydration the chemical shift δ_{Na}, taken as the peak maximum, changes linearly from 0.27 ppm at 25°C to 1.56 ppm at 105°C

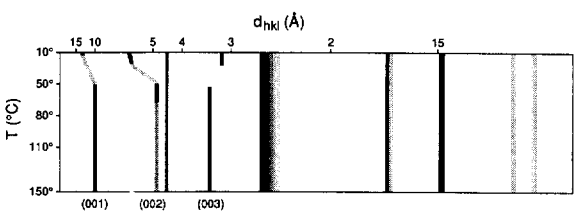

Figure 1. Heating stage X-ray powder diffraction pattern in the temperature range 20° to 150°C (Guinier film). Indicated are the (001) reflections.

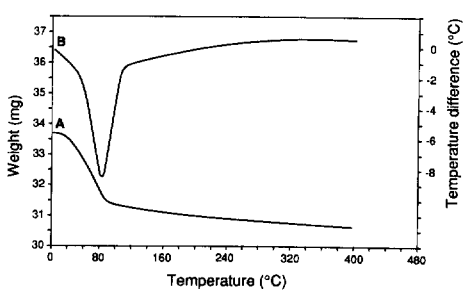

Figure 2. Thermal analysis results for synthetic Na-beidellite: A) TGA, B) DTA.

https://doi.org/10.1346/CCMN.1992.0400510 Published online by Cambridge University Press

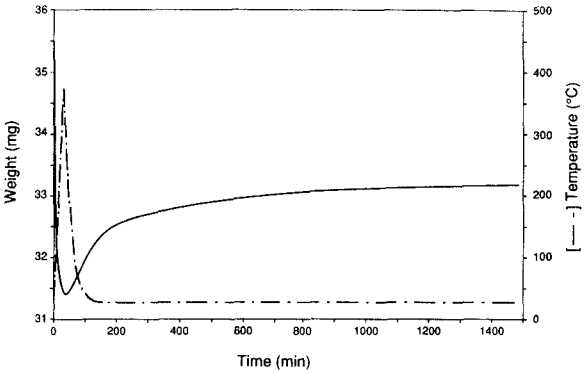

Figure 3. Resorption of water following dehydration at 400°C and subsequent cooling to room temperature in the TGA apparatus. The increase in weight represents 3 molecules H_2O per Na^+. Solid line = weight in mg, y-axis values on left; dashed line = temperature profile, y-axis values on right.

(Figure 5). The linewidth at half height (FWHH) decreases simultaneously from 33.6 to 20.3 Hz (Table 2).

In the ^{27}Al spectra two resonances are recognized with chemical shifts, δ_{Al} of approximately 3.9 ppm and 69.9 ppm (Figure 4B), representing $^{[6]}Al$ and $^{[4]}Al$, respectively, in the Na-beidellite structure (Kloprogge *et al.*, 1990a). The $^{[6]}Al$ resonance exhibits a right-side asymmetry. Dehydration has no influence on the chemical shifts of both $^{[4]}Al$ and $^{[6]}Al$. The FWHH of the tetrahedral Al resonance remains constant, whereas that of the octahedral one decreases from 895 Hz at 25°C to 692 Hz at 105°C (Table 2). The ^{29}Si spectra exhibit signals at −92.7 ppm, −88.4 ppm, and −82.3 ppm assigned to Si surrounded by zero, one, and two Al in the neighbouring tetrahedra. A small shift, approximately 0.3 ppm, towards more negative values is observed upon heating. The peak width at half height increases slightly from 736 Hz to 796 Hz.

DISCUSSION

The basal spacing of Na-beidellite (12.54Å) indicates the presence of a monomolecular layer of water in the interlayer, in which each Na^+ atom, surrounded by water molecules, is positioned very close to the center of the interlayer space (Kawano and Tomita, 1991). The decrease of the basal spacing to 9.98 Å during dehydration below 85°C indicates the break up of the monomolecular layer. The TGA profile displays a major loss of 6.6 wt. %, which is equivalent to 2.9 moles of water per mole of $Na_{0.7}$-beidellite, or representing 4 molecules of water per Na^+ atom. Upon heating to 400°C the dehydration of the Na-beidellite produces a constant basal spacing of 9.98 Å and slowly progresses to a total weight loss of 9.2%, which is equivalent to 6 molecules of water per Na^+ atom. Na surrounded by 6 water molecules is known to have an octahedral coordination which would result in the development of

Table 2. ^{23}Na and ^{27}Al MAS-NMR chemical shifts δ (ppm) and full width at half height FWHH (Hz) as a function of dehydration temperature.

	^{23}Na		$^{27[4]}Al$		$^{27[6]}Al$	
T (°C)	δ	FWHH	δ	FWHH	δ	FWHH
25	0.266	33.6	69.9	488	3.9	895
45	0.632	30.5	69.9	488	3.9	827
65	0.899	25.4	69.9	488	3.9	786
85	1.223	24.4	69.9	488	3.9	732
105	1.555	20.3	69.9	488	3.9	692

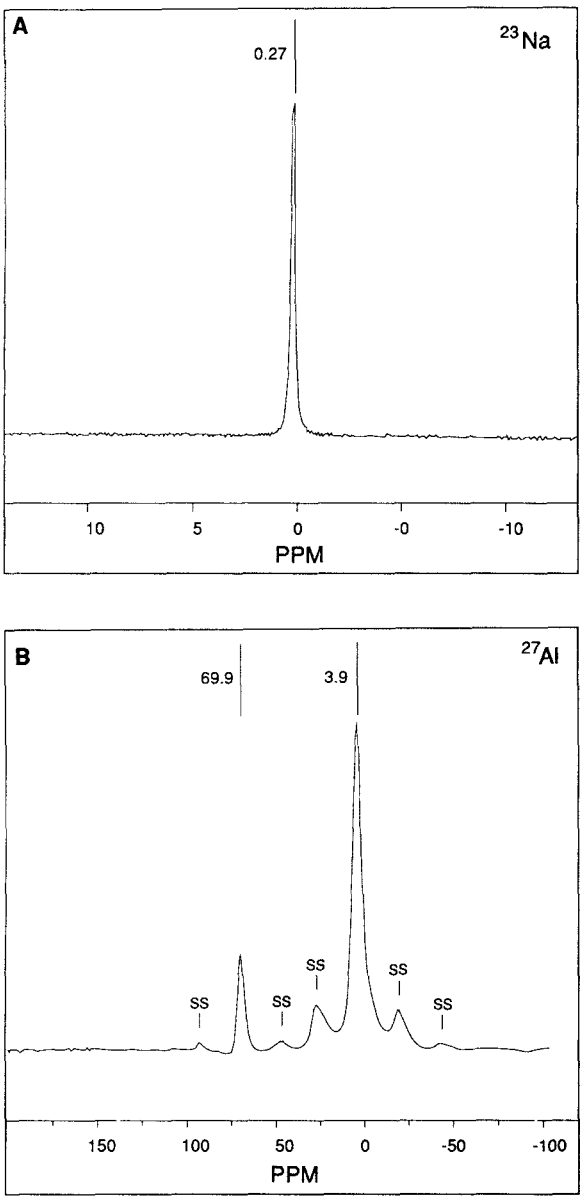

Figure 4. Solid-state MAS-NMR spectra of synthetic Na-beidellite: A) ^{23}Na and B) ^{27}Al. SS signifies spinning sidebands.

https://doi.org/10.1346/CCMN.1992.0400510 Published online by Cambridge University Press

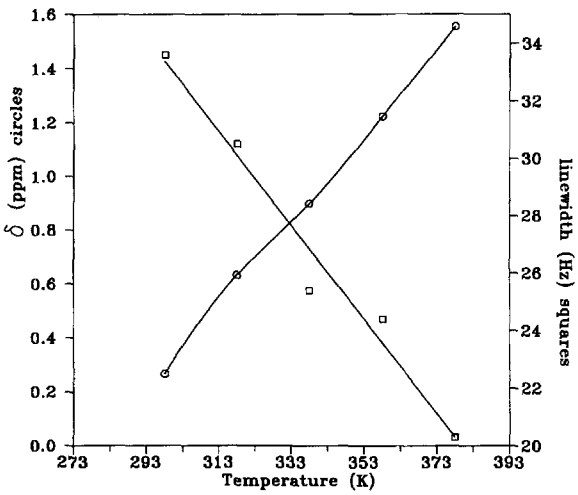

Figure 5. Chemical shift δ (open circles) and the linewidth at half height (FWHH) (solid squares) of ^{23}Na as function of the dehydration temperature.

a two-layer hydrate of Na-beidellite having a basal spacing of 14–15 Å. At the applied relative humidity of 60%, capillary condensation in the interaggregate and intraaggregate pores of the beidellite may well be initiated and account for some of the adsorbed water (Touret *et al.*, 1990). This explains the basal spacing of 12.54 Å of a one-layer hydrate beidellite.

The synthetic Na-beidellite exhibits a continuous dehydration between 85° and 400°C, which, smoothly, changes into dehydroxylation above approximately 400°C (Kloprogge *et al.*, 1990b). According to Koster van Groos and Guggenheim (1987) the second dehydration step of montmorillonite terminates at approximately 260°C. The difference in dehydration behaviour of beidellite and montmorillonite is attributed to a difference in the clay sheets, especially the distribution of electrostatic charge affecting the configuration of the interlayer region. In montmorillonite the negative charge originates mainly from octahedral M^{2+} substitution for Al^{3+} and, therefore, is distributed over all oxygens in the tetrahedral layer. In beidellite, on the other hand, the negative charge is due to tetrahedral Al^{3+} substitution for Si^{4+}. The negative charge thus is mainly located on the three basal oxygens of the Al^{3+} substituted tetrahedron, resulting in a more strongly localized interaction with the adjacent interlayer region. Hence, one would expect strong electric field gradient (EFG) effects in the Al, especially during dehydration. The unchanged linewidth of the tetrahedral Al NMR peak, however, indicates that the EFG must remain unmodified (Luca *et al.*, 1989).

The dehydration experiments have shown that the basal spacing is 9.98 Å after the first dehydration stage, with still two water molecules per Na^+ atom present. This suggests a reorganization of the geometry of the remaining interlayer water around the Na^+. The uptake of one additional molecule of water per Na^+ is sufficient to restore the original geometry and a basal spacing of 12.44 Å. The dimensions of the water molecules force the Na-beidellite to assume the original basal spacing immediately after the start of the water resorption.

The chemical shift of the ^{23}Na resonance at 25°C of the Na-beidellite is very close to that of Na^+ in solution, indicating a similar environment. The rapid motion of water molecules around the Na^+ causes an efficient relaxation, as previously reported for ^{113}Cd in montmorillonite (Bank *et al.*, 1989). Therefore, a very short repetition delay of 0.15 s suffices for the ^{23}Na MAS-NMR spectra. The change of the local environment due to the removal of 4 water molecules and the collapse of the interlayer space from approximately 3 Å to 0.5 Å upon dehydration seems to make the peak maxima more positive. It has to be kept in mind that exact interpretation of the observed differences in chemical shift is difficult due to the influence of the motionally averaged environment of the Na^+. The chemical shift differences point to a steadily increasing influence of the tetrahedral sheet and especially the Al^{3+} substituted tetrahedra on the Na^+ site. The sharp single resonance of ^{23}Na reflects a relatively small quadrupole coupling constant (QCC = e^2qQ/h) and, therefore, a high local symmetry.

Neglecting the influence of the motionally averaged environment, an approximate quadrupole coupling constant can be calculated from the measured linewidth at half height (FWHH) by applying the formula for the linewidth postulated by Akitt (1989) from the calculations of Kentgens *et al.* (1983):

$$\text{FWHH} = \frac{\upsilon_Q^2}{3\upsilon_0}$$

in which $\upsilon_Q = 3e^2qQ/h2I(2I - 1)$ (e^2qQ/h = QCC in kHz, ^{23}Na spin I = 3/2) and υ_0 is the Larmor frequency (in kHz). At 25°C the quadrupole coupling constant (QCC) is approximately 230 kHz. This value is only slightly higher than that of solid NaCl (approximately 117–135 kHz at 25°C based on a FWHH of 3–4 ppm at 39.7 MHz, Meadows *et al.*, 1982) which has a very high local symmetry with each Na^+ in an octahedron of six Cl^-. It is lower than the QCC of $NaNO_3$ (≈300 kHz) or $NaNO_2$ (≈1.1 MHz, Engelhardt and Michel, 1987).

Modification of the local environment of the Na^+ caused no changes in the ^{27}Al MAS-NMR chemical shifts for both $^{[4]}Al$ and $^{[6]}Al$ in the first dehydration interval. Applying the same relation for the calculation of the quadrupole coupling constants of the $^{[4]}Al$ and $^{[6]}Al$ results in values of 2.9 MHz and 3.9 MHz, respectively. The value obtained for the octahedral resonance is rather questionable, because the asymmetry of the resonance may arise from several sites with the same coordination and similar chemical shift, but different quadrupole coupling constants and asymmetry parameters η. Woessner (1989) reported slightly greater

linewidths for natural beidellite from the Black Jack Mine, Idaho: 4.2 ppm (547 Hz) and 4.4 ppm (573 Hz) for tetrahedral (δ = 70.0 ppm) and octahedral (δ = 3.1 ppm) Al, respectively. Based on the Kunwar *et al.* (1984) formula,

$$\delta(\text{ppm}) = -6 \times 10^3(e^2qQ/h\upsilon_0)^2(1 + \tfrac{1}{3}\eta^2),$$

in which η is the asymmetry parameter, Woessner (1989) calculated a SOQE (second order quadrupole effect), which is equal to $(e^2qQ/h)(1 + \frac{1}{3}\eta^2)^{1/2}$, for the tetrahedral resonance of 2.54 MHz. The asymmetric octahedral resonance was described by a peak with $\eta = 0$ and QCC = 5.6 MHz and one with SOQE = 2.1 MHz. In general the SOQE for $^{[4]}$Al increases with increasing tetrahedral substitution resulting from a tetrahedral sheet distortion (Ghose and Tsang, 1973). In comparison with the Black Jack beidellite, the synthetic beidellite has a slightly lower tetrahedral Al substitution ($^{[4]}$Al/Si = 0.151 and 0.096, respectively) and thus a lower SOQE is expected. Based on the QCC of 2.9 MHz and assuming $\eta = 0$, the SOQE is slightly higher than the value of 2.49 MHz observed by Woessner (1989). The difference in QCC may be caused by a poorer crystallinity of the synthetic beidellite.

The decreasing linewidths of the ^{23}Na and ^{27}Al resonances are caused by second order quadrupole effects due to heating in the NMR apparatus. Quadrupole relaxation is partly governed by the correlation time of the EFG. This term is temperature dependent and decreases with increasing temperature, thus narrowing the linewidth of quadrupolar nuclei (Akitt, 1989).

Upon dehydration small monovalent interlayer cations, such as Na^+, can take up position in the hexagonal cavities close to the Al^{3+} substituted tetrahedra (Kawano and Tomita, 1991), forming chains parallel to the b-axis. The Na^+ is thereby bonded to only one tetrahedral sheet. The alternate chain of hexagonal cavities is left vacant (Güven, 1988). The positioning of Na^+ in the hexagonal cavities explains the high local symmetry and change in chemical shift observed by ^{23}Na MAS-NMR after the first dehydration step.

The very small changes in the ^{29}Si chemical shift and linewidth suggest small changes in the distribution of Si–O–Si/Al bond angles due to the movement of Na^+ to the hexagonal cavities. It also agrees with the decrease of the interlayer space to 0.5 Å, which is even smaller than the effective radius of Na^+ (e.g., 0.99 Å for $^{[4]}$Na and 1.39 Å for $^{[12]}$Na in chalcogenides and halides, Shannon, 1976). In paragonite, $Na_2Al_6Si_6O20(OH)_4$, the sodium ions are similarly situated in the hexagonal cavities having an octahedral coordination with an average distance Na–O of 2.63 Å (Sidorenko *et al.*, 1977a, 1977b; Lin and Bailey, 1984). Furthermore, computer calculations of XRD intensities for beidellite and dehydrated beidellite with interlayer Na^+ positioned on the same level as the basal oxygen of the tetrahedral layer show exactly the same behaviour as observed with HT-XRD.

The size of a water molecule combined with the relatively high dehydration temperature of the remaining two water molecules without any further decrease in basal spacing indicate that the water molecules are more strongly bonded to the interlayer Na^+ and may be located in one or two hexagonal cavities. This is supported by the fact that the enthalpy per water molecule for the second dehydration step in montmorillonites is clearly higher than that of the first step (Koster van Groos and Guggenheim, 1987).

The ordering of the Na^+ in chains due to the distribution of Al over the tetrahedral sheet following the Loewenstein avoidance rule (Loewenstein, 1954) also has implications for the distribution of pillaring complexes such as the tridecameric polymer Al_{13}, in pillared clays. The pillars are probably situated directly between two hexagonal rings from two adjacent tetrahedral sheets containing substituted Al, resulting in a rather regular hexagonal distribution of the pillars. After calcination these pillars are presumably anchored to the apical oxygen of an inverted aluminum tetrahedron pointing out into the interlamellar space from the tetrahedral sheet, as suggested by Plee *et al.* (1985) based on ^{27}Al and ^{29}Si MAS-NMR.

CONCLUSION

The data consistently point to a model in which the Na^+ in Na-beidellite exhibits a behaviour comparable to that of Na^+ in solution with a rapid motion of the water molecules around the Na^+, as evidenced by the rapid relaxation. The very high local symmetry is supported by the small QCC of 113 kHz. During the first step of the dehydration, which proceeds below 85°C, four of the six water molecules are easily removed, resulting in a decrease of the basal spacing from 12.54 Å to 9.98 Å. The total loss of 6 water molecules per Na^+ during dehydration and the observation of a basal spacing of a one-layer hydrate beidellite indicate that not only interlayer hydrate complexes are formed but also capillary condensation in the pores takes place. After the first dehydration step, the remaining two water molecules and the Na^+ are relocated in chains of hexagonal cavities near the Al^{3+} substituted tetrahedra and no further decrease of the basal spacing can be observed. The Na^+ is situated within the hexagonal cavity, because the interlayer space of 0.5 Å is smaller than the effective radius of the Na^+ ion. This relocation results in a slightly stronger bonding of the water molecules to the interlayer Na^+ as evidenced by the high dehydration temperature of 400°C.

ACKNOWLEDGMENTS

The authors wish to thank H. M. V. C. Govers for the HT-XRD patterns, T. Zalm for the TGA, DTA, and DSC curves. They are especially thankful to G. Nachtegaal for the technical assistance at the NWO-SON HF-NMR facility at Nijmegen. We also thank M. K. Titulaer, J. J. van Beek, P. J. Dirken, and R.

Vogels for critically reviewing the manuscript. N. Güven is especially thanked for his critical review and discussion of the modes of hydration of smectites.

REFERENCES

Akitt, J. W. (1989) Multinuclear studies of aluminum compounds: *Progr. NMR Spectr.* **21,** 1–149.

Bank, S., Bank, J., and Ellis, P. D. (1989) Solid-state ^{113}Cd nuclear magnetic resonance study of exchanged montmorillonite: *J. Phys. Chem.* **93,** 4847–4855.

Chu, P. J., Gerstein, B. C., Nunan, J., and Klier, K. (1987) A study by solid-state NMR of ^{133}Cs and ^{1}H of a hydrated and dehydrated cesium mordenite: *J. Phys. Chem.* **91,** 3588–3592.

Engelhardt, G., and Michel, D. (1987) *High-resolution Solid-state NMR of Silicates and Zeolites:* Wiley, New York, 485 pp.

Ghose, S., and Tsang, T. (1973) Structural dependence of quadrupole coupling constant e^2qQ/h for ^{27}Al and crystal field parameter D for Fe^{3+} in aluminosilicates: *Amer. Mineral.* **58,** 748–755.

Güven, N. (1988) Smectites: in *Hydrous Phyllosilicates (Exclusive of Micas),* S. W. Bailey, ed., *Reviews in Mineralogy* **19,** Mineralogical Society of America, Washington, D.C., 497–559.

Hamilton, D. L., and Henderson, C. M. B. (1968) Preparation of silicate compositions by a gelling method: *Mineral. Mag.* **36,** 832–838.

Janssen, R., Dols, P. P. M. A., Tijink, G. A. H., and Veeman, W. S. (1989a) High temperature NMR of zeolites: in *Zeolites: Facts, Figures, Future. Stud. Surf. Sci. and Catal. 49 A/B,* P. A. Jacobs and R. A. van Santen, eds., Proc. 8th Int. Zeolite Conf. Amsterdam 1989, Elsevier, Amsterdam, 609–614.

Janssen, R., Tijink, G. A. H., Veeman, W. S., Maesen, T. L. M., and van Lent, J. F. (1989b) High temperature NMR study of zeolite Na-A: Detection of a phase transition: *J. Phys. Chem.* **93,** 899–904.

Kawano, M., and Tomita, K. (1991) X-ray powder diffraction studies on the rehydration properties of beidellite: *Clays & Clay Minerals* **39,** 77–83.

Kentgens, A. P. M., Scholle, K. F. M. G. J., and Veeman, W. S. (1983) Effect of hydration on the local symmetry around aluminum in ZSM-5 zeolites studied by aluminum-27 nuclear magnetic resonance: *J. Phys. Chem.* **87,** 4357–4360.

Kirkpatrick, R. J. (1988) MAS NMR spectroscopy of minerals and glasses: in *Spectroscopic Methods in Mineralogy and Geology,* F. C. Hawthorne, ed., *Reviews in Mineralogy* **18,** Mineralogical Society of America, Washington, D. C., 341–403.

Kirkpatrick, R. J., Kinsey, R. A., Smith, K. A., Henderson, D. M., and Oldfield, E. (1985) High resolution solid-state sodium-23, aluminum-27, and silicon-29 nuclear magnetic resonance spectroscopic reconnaissance of alkali and plagioclase feldspars: *Amer. Mineral.* **70,** 106–123.

Kloprogge, J. T., van der Eerden, A. M. J., Jansen, J. B. H., and Geus, J. W. (1990a) Hydrothermal synthesis of Na-beidellite: *Geologie en Mijnbouw* **69,** 351–357.

Kloprogge, J. T., Jansen, J. B. H., and Geus, J. W. (1990b) Characterization of synthetic Na-beidellite: *Clays & Clay Minerals* **38,** 409–414.

Koster van Groos, A. F., and Guggenheim, S. (1984) The effect of pressure on the dehydration reaction of interlayer water in Na-montmorillonite (SWy-1): *Amer. Mineral.* **69,** 872–879.

Koster van Groos, A. F., and Guggenheim, S. (1986) Dehydration of K-exchanged montmorillonite at elevated temperatures and pressures: *Clays & Clay Minerals* **34,** 281–286.

Koster van Groos, A. F., and Guggenheim, S. (1987) Dehydration of a Ca- and a Mg-exchanged montmorillonite (SWy-1) at elevated pressures: *Amer. Mineral.* **72,** 292–298.

Kunwar, A. C., Thompson, A. R., Gutowsky, H. S., and Oldfield, E. (1984) Solid state aluminum-27 NMR studies of tridecameric Al-oxo-hydroxy clusters in basic aluminum selenate, sulfate, and the mineral zunyite: *J. Magn. Reson.* **60,** 467–472.

Lin, C.-Y., and Bailey, S. W. (1984) The crystal structure of paragonite-$2M_1$: *Amer. Mineral.* **69,** 122–127.

Loewenstein, W. (1954) The distribution of aluminum in the tetrahedra of silicates and aluminates: *Amer. Mineral.* **57,** 1089–1108.

Luca, V., Cardile, C. M., and Meinhold, R. H. (1989) High-resolution multinuclear study of cation migration in montmorillonite: *Clay Miner.* **24,** 115–119.

Meadows, M. D., Smith, K. A., Kinsey, R. A., Rothgeb, T. M., Skarjune, R. P., and Oldfield, E. (1982) High-resolution solid-state NMR of quadrupolar nuclei: *Proc. Nat. Acad. Sci. USA* **79,** 1351–1355.

Oestrike, R., Yang, W.-H., Kirkpatrick, R. J., Hervig, R. L., Navrotsky, A., and Montez, B. (1987) High resolution ^{23}Na, ^{27}Al, and ^{29}Si NMR spectroscopy of framework aluminosilicate glasses: *Geochim. Cosmochim. Acta* **51,** 2199–2209.

Plee, D., Borg, F., Gatineau, L., and Fripiat, J. J. (1985) High-resolution solid-state ^{27}Al and ^{29}Si nuclear magnetic resonance study of pillared clays: *J. Am. Chem. Soc.* **107,** 2362–2369.

Shannon, R. D. (1976) Revised effective ionic radii and systematic studies of interatomic distances in halides and chalcogenides: *Acta Crystallogr.* **A32,** 751–767.

Sidorenko, O. V., Zvyagin, B. B., and Soboleva, S. V. (1977a) Refinement of the crystal structure of $2M_1$ paragonite by the method of high-voltage electron diffraction: *Sov. Phys./Amer. Inst. Phys. Crystallography* **22,** 554–556 (translated from *Kristallografija* **22,** 971–975, 1977).

Sidorenko, O. V., Zvyagin, B. B., and Soboleva, S. V. (1977b) The crystal structure of 3T paragonite: *Sov. Phys./Amer. Inst. Phys. Crystallography* **22,** 557–560 (translated from *Kristallografija* **22,** 976–981, 1977).

Touret, O., Pons, C. H., Tessier, D., and Tardy, Y. (1990) Etude de repartition de l'eau dans les argiles Mg^{2+} aus fortes teneurs en eau: *Clay Miner.* **25,** 217–233.

Tuttle, O. F. (1949) Two pressure vessels for silicate-water studies: *Geol. Soc. Amer. Bull.* **60,** 1727–1729.

Weiss, C. A., Kirkpatrick, R. J., and Altaner, S. P. (1990a) The structural environment of cations adsorbed onto clays: ^{133}Cs variable-temperature MAS NMR spectroscopic study of hectorite: *Geochim. Cosmochim. Acta* **54,** 1655–1669.

Weiss, C. A., Kirkpatrick, R. J., and Altaner, S. P. (1990b) Variations in interlayer cation sites of clay minerals as studied by ^{133}Cs MAS nuclear magnetic resonance spectroscopy: *Amer. Mineral.* **75,** 970–982.

Woessner, D. E. (1989) Characterization of clay minerals by ^{27}Al nuclear magnetic resonance spectroscopy: *Amer. Mineral.* **74,** 203–215.

Yang, W.-H., Kirkpatrick, R. J., and Henderson, D. M. (1986) High resolution ^{29}Si, ^{27}Al, and ^{23}Na NMR spectroscopic study of Al-Si disordering in annealed albite and oligoclase: *Amer. Mineral.* **71,** 712–726.

(Received 3 March 1992; accepted 21 September 1992; Ms. 2209)